

Synthesis, Solid-State Analyses, and Anion-Binding Properties of *meso*-Aryldipyrroin-5,5'-diylbis(phenol) and -bis(aniline) Ligands

Laurent Copey,^[a] Ludivine Jean-Gérard,^[a] Eric Framery,^[a] Guillaume Pilet,^[b] and Bruno Andrioletti*^[a]

Dedicated to Professor Max Malacria on the occasion of his 65th birthday

Keywords: Dipyrrromethenes / Structure elucidation / Hydrogen bonds / Anion binding / Substituent effects

The design of new molecular scaffolds for the selective recognition or transport of anions is often critical, because subtle changes in the substitution pattern may drastically impact the targeted properties. Herein, detailed spectroscopic and X-ray crystal-structure analyses were used to investigate the effect of the substitution pattern of a new series of N₂O₂ or N₄ anion sensors. Our study evidences two distinct *in-in* and *in-out* conformations depending on the nature of the substituent (e.g., phenol vs. aniline). Interestingly, because

of intramolecular hydrogen bonds involving the –OH or the –NH₂ functions, the dipyrroin subunit only acts as a scaffold and does not participate in the anion binding. Furthermore, the nature of the *meso* substituent was not critical, as similar binding affinities were measured for *meso*-C₆H₅ or *meso*-C₆F₅ ligands. Hence, the *meso* position can be further modified without any noticeable changes to the electron density on the dipyrromethene subunit.

Introduction

Despite a tremendous amount of work over the past decades, the development of easy-to-access ligands still constitutes a major issue for synthetic chemists. Indeed, the time-consuming preparation of elaborate scaffolds sometimes leads to disappointing (catalytic) activities or molecular properties. In this context, the design of new structures is still challenging and highly desirable. Recently, 2-aryldipyrromethene-based ligands underwent a renewed interest because of their remarkable binding and photophysical properties. Hence, we^[1] and others^[2] have reported the synthesis and applications of dipyrroindiphenol ligands (DPPH₃ or N₂O₂-type ligands) featuring the dipyrromethene unit of a porphyrin and the salicylimine moiety of a salen. Interestingly, the synthetic access to DPPH₃ ligands appeared easier than that to porphyrins, but the catalytic activity remained below expectations.^[1] The presence of both a conju-

gated system (reporter) and H-bond donors on the DPPH₃ scaffold prompted us to develop a series of ligands with similar features. To this end, we undertook the preparation of dipyrroindianiline systems (Figure 1).

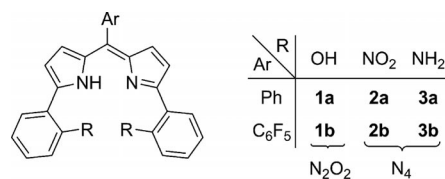


Figure 1. Structures of the N₂O₂ and N₄ ligands.

Results and Discussion

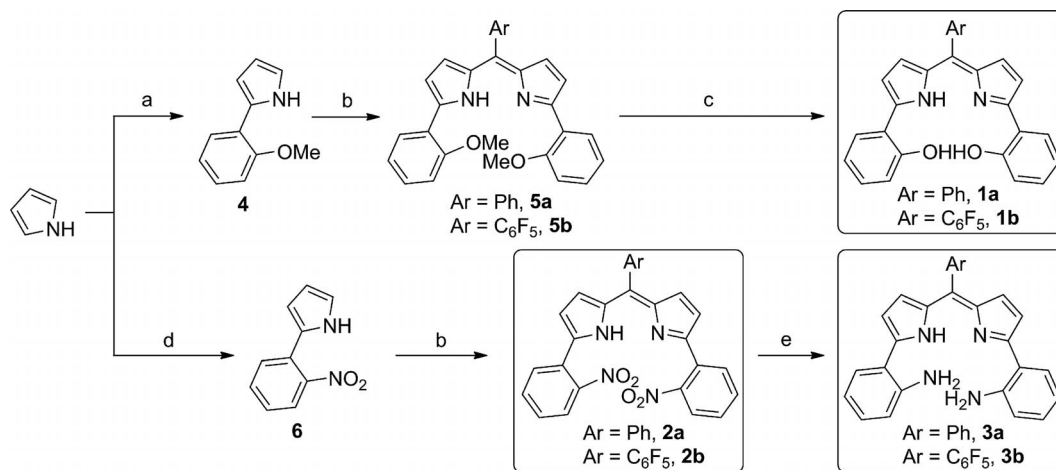
I. Synthesis

The two N₂O₂ ligands **1a** and **1b** have already been synthesized by our group^[1] and others^[2] by applying the pioneering work of Burgess et al.^[3] The chosen strategy begins with the formation of 2-(2-methoxyphenyl)-1*H*-pyrrole (**4**) by a palladium-catalyzed arylation of the pyrrole anion with 2-chloroanisole (Scheme 1).^[4] After condensation with benzaldehyde or its perfluorinated analogue and oxidation of the resulting dipyrromethanes, demethylation of the dipyrroins **5a** and **5b** was performed with boron tribromide in CH₂Cl₂.^[2] The expected dipyrroindiphenols **1a** and **1b** were formed in global yields of 60 and 36% over four steps when

[a] ICBMS-UMR 5246 Université Claude Bernard Lyon, Equipe de Catalyse, Synthèse et Environnement (CASYEN), Domaine Scientifique de la Doua-Bât. Curien/CPE, 2^e étage aile C, 43 Boulevard du 11 Novembre 1918, 69622 Villeurbanne CEDEX, France
E-mail: bruno.andrioletti@univ-lyon1.fr
http://www.icbms.fr/casyen/andrioletti

[b] Laboratoire des Multimatériaux et Interfaces (LMI), UMR 5615 CNRS-Université Claude Bernard Lyon, 43 Boulevard du 11 Novembre 1918, 69622 Villeurbanne CEDEX, France

Supporting information for this article is available on the WWW under <http://dx.doi.org/10.1002/ejoc.201402446>.



Scheme 1. (a) (i) NaH (4 equiv.), THF, (ii) ZnCl₂ (4 equiv.), (iii) Pd(OAc)₂ (0.5 mol-%), JohnPhos (0.5 mol-%), 2-chloroanisole (1 equiv.), 65 °C, 24 h, 93%; (b) (i) ArCHO (0.5 equiv.), TFA (10 mol-%), CH₂Cl₂, room temp., 4 h for **5a**, 1 h for **5b**, 11 h for **2**, (ii) DDQ, 1 h, 70% (**5a**) or *p*-chloranil, 2–4 h, 77% (**5b**), 55% (**2a**), 70% (**2b**); (c) BBr₃ (4 equiv.), CH₂Cl₂, 12 h, room temp., 90 (**1a**) and 49% (**1b**); (d) 1-bromo-2-nitrobenzene (0.25 equiv.), Cs₂CO₃ (0.5 equiv.), reflux, 3 d, 92%; (e) 10% Pd/C (10 mol-%), NH₂NH₂·H₂O (20 equiv.), EtOH, reflux, 3 d, 78% (**3a**) or 5% Lindlar catalyst (5 mol-%), H₂ (1 atm), MeOH, room temp., 14 h, 76% (**3b**).

benzaldehyde and pentafluorobenzaldehyde were used as the partner, respectively. The undesired formation of boron complexes (as described by Ikeda et al.)^[2a] during the final deprotection of the *meso*-(pentafluorophenyl)dipyrin **5b** lowered the overall yield of **1b**. Similarly, the preparation of four new N₄ ligands by using 2-(2-nitrophenyl)-1*H*-pyrrole (**6**) as the main building block was performed by a strategy also used by Alešković et al. for the preparation of *meso*-adamantyl analogues.^[5] The palladium-catalyzed approach previously used for the preparation of **4** proved to be unsuccessful with the strongly electron-deficient 1-bromo-2-nitrobenzene. Conversely, the synthesis of **6** was efficiently performed in 66% yield by a metal-free nucleophilic aromatic substitution of 1-bromo-2-nitrobenzene with pyrrole.^[6] Next, the corresponding dipyrromethenes **2a** and **2b** were prepared according to our previous procedures in 55 and 70% yield, respectively. After optimization, it appeared that the amino ligands **3a** and **3b** could be obtained by reduction of the nitro groups in 78 and 76% yield, respectively, by using two different protocols depending on the nature of the *meso* substituent. The reduction of the nitro groups of the *meso*-phenyl ligand **2a** was performed efficiently with hydrazine hydrate and palladium on charcoal,^[7] whereas the reduction of the *meso*-pentafluorophenyl ligand **2b** was performed by using Lindlar catalyst under hydrogen.^[8]

II. Characterization

Compounds **1–3** were fully characterized by the standard techniques. Interestingly, several single crystals suitable for X-ray diffraction analyses were grown by slow concentration of solutions of the ligands in dichloromethane (DCM). The solid-state analyses revealed common trends between the family members. Compounds **2a**^[9] (Figure 2a) and **2b**^[10] (Figure 2b) are similar and only differ in the substitution patterns of the *meso*-aryl substituent. In both solid-state

crystal structures, the –NO₂ groups are in an “*in-in*” conformation (Figure 3). In addition, as is commonly observed in dipyrromethene structures,^[11] the NH pyrrole moiety forms a hydrogen bond with the sp²-hybridized nitrogen atom of the second pyrrole ring.

In **2a**, no intermolecular hydrogen-bond network is evidenced, and the structural cohesion is ensured by weak interactions. On the contrary, the X-ray solid-state analysis of **2b** reveals that the fluorine atoms form intra- and intermolecular F⋯H hydrogen bonds (Figure 2b) with the β-pyrrole hydrogen atoms and the nitrophenyl groups of neighboring molecules. Interestingly, the substitution pattern of the *meso*-aryl substituent does not influence the dihedral angle formed by the *meso*-aryl substituent and the dipyrromethene mean plane (69.5 and 67.8° for **2a** and **2b**, respectively). Owing to the presence of intermolecular F⋯H hydrogen bonds, the crystal structure of **2b** can be described as a 2D polymer parallel to the *bc* plane of the unit cell (Figure 2c).

Noticeably, the X-ray crystal structure of **3b**^[12] reveals that one of the anilino groups has rotated, and this results in an “*in-out*” conformation in the solid state (Figure 4, left). Consequently, the formation of a remarkable intermolecular hydrogen-bond network involving the –NH₂ groups is evidenced (Figure 4, right). This observation contrasts with what is observed for the **2b** analogue. It is also worth noting that the angle between the *meso*-C₆F₅ substituent and the dipyrromethene mean plane (85.1°) is slightly larger than those of the related structures described above. This can be correlated to the F⋯H(NH) hydrogen-bond network or to the difference in size between the NO₂ and the NH₂ substituents. The intermolecular F⋯H hydrogen bonds form planes in the *ac* plane of the unit cell, which stack parallel along the [100] direction (Figure 4, right). The whole cohesion between the planes is ensured by weak van der Waals interactions.

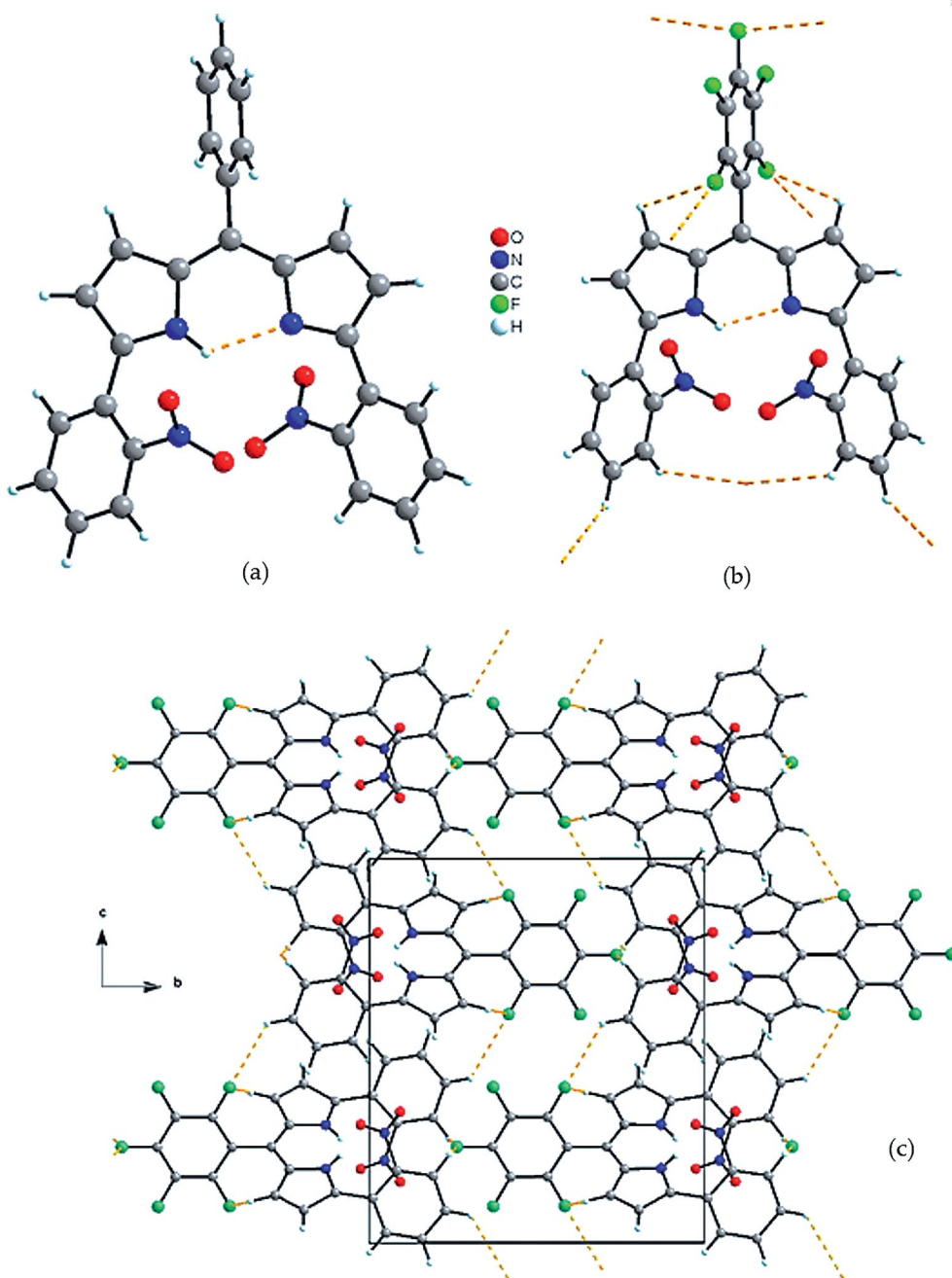


Figure 2. Structures of (a) **2a** and (b) **2b** with intra- and intermolecular F \cdots H hydrogen bonds represented in orange dashed lines. (c) Crystal packing of **2b**, which forms planes perpendicular to the *a* axis of the unit cell owing to intermolecular F \cdots H bonds. For clarity, only hydrogen atoms involved in hydrogen bonds are represented.

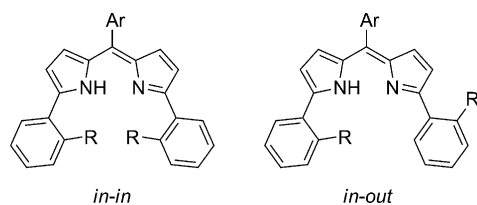


Figure 3. Two different conformations of the N₂O₂ or N₄ ligands.

On the basis of this information and as the propensity to form hydrogen bonds is a cornerstone for the development

of anion receptors or transporters,^[13] we decided to evaluate the anion-binding properties of our series of ligands. Indeed, these dipyrin ligands bear promising features including hydrogen-bond donors and a conjugated system that could act as a reporter. These features have been recognized as critical for the development of naked-eye anion sensors.^[14] Indeed, it is well acknowledged that pyrrole derivatives can act as anion receptors through their acidic NH protons.^[15] In addition, in the present case, the pheno^[16] and aniline^[5] substituents could also provide additional hydrogen binding sites. Thus, it was envisioned that the

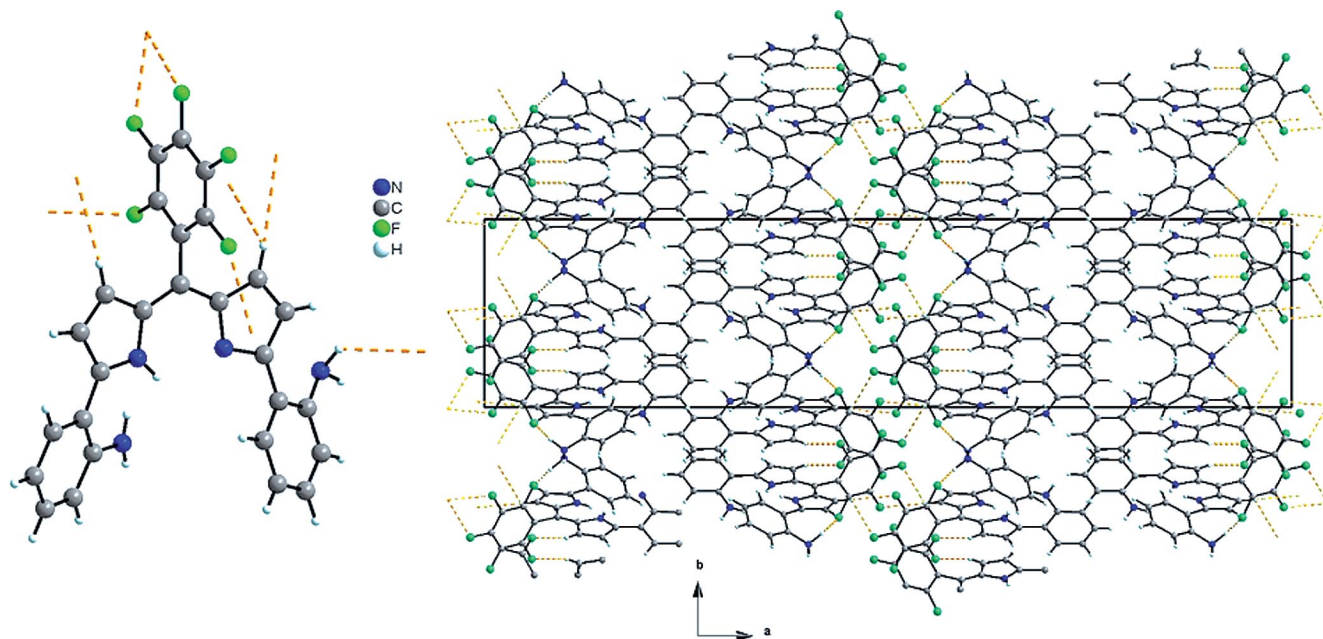


Figure 4. Left: structure of **3b** with F...H hydrogen bonds in orange dashed lines. Right: crystal-structure packing with planes of molecules formed parallel to the *ab* plane of the unit cell.

newly designed dipyrins would host anions thanks to a convergent hydrogen-bond network.

III. Anion-Binding Studies

Solution studies with the ligands and various anions added as tetrabutylammonium (TBA) salts were conducted by UV/Vis spectroscopy or by ^1H NMR titrations in $[\text{D}_6]$ -acetone when no noticeable change was detected in the UV/Vis spectra upon addition of anions or when insights into the binding mode were sought. Standard nonlinear regression treatment of the resulting data permitted the calculation of the stability constants, which are summarized in Table 1 (see also the Supporting Information). Several general conclusions can be drawn from the data in Table 1.

Table 1. Stability constants K_a (M^{-1}) determined in $[\text{D}_6]$ -acetone by ^1H NMR titration and in acetone by UV/Vis spectroscopy at 298 K.

| Entry | Compound | F ⁻ /AcO ⁻ /BzO ⁻ | Cl ⁻ | Br ⁻ | HSO ₄ ⁻ | NO ₃ ⁻ |
|-------|-----------|--|-----------------|-----------------|-------------------------------|------------------------------|
| 1 | 1a | >10 ⁶ | 47 | 16 | 36 | 10 |
| 2 | 1b | >10 ⁶ | 89 | 11 | 42 | 29 |
| 3 | 2a | >10 ⁶ | | | n.d. ^[a,b] | |
| 4 | 2b | >10 ⁶ | | | n.d. ^[a,b] | |
| 5 | 3a | >10 ⁶ | 85 | 18 | <10 ^[b] | 27 |
| 6 | 3b | >10 ⁶ | 267 | 33 | <10 ^[b] | <10 ^[b] |

[a] No change in the ^1H NMR spectrum was observed. [b] Titration performed in CDCl_3 .

Interactions between Dipyrromethene-Based Receptors and Basic Anions

The anion-binding affinities of receptors **1–3** with F⁻, AcO⁻, and BzO⁻ anions were first evaluated by UV/Vis

spectroscopy (Figure 5). A representative behavior is illustrated with **3b**. In the absence of anions, the absorption maximum peak appears at 544 nm for **3b**. Upon the addition of F⁻ ions, a bathochromic and hyperchromic shift was observed with the disappearance of the absorption band at 544 nm and the appearance of a new intense band at 601 nm. Similar behaviors were observed for dipyrromethenes **1a**, **1b**, and **3a** (see Supporting Information). As can be anticipated from these UV/Vis data, a color change from red to blue also occurs upon the addition of anions to the solution of the receptor **3b**. Considering the strong basicity of the studied anions, this behavior was attributed to deprotonation of the ligand. This hypothesis was further confirmed by adding increasing amounts of tetrabutyl-

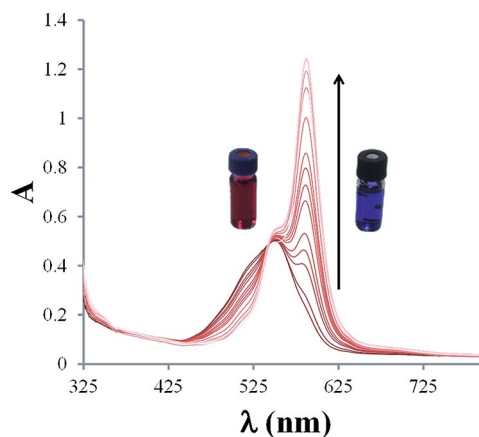


Figure 5. Typical evolution of the UV/Vis spectrum of **3b** upon the addition of increasing amounts of TBAF in acetone. Red solution: protonated form; blue solution: deprotonated form.

ammonium hydroxide to a solution of the ligands. As anticipated, the same color change and a similar behavior in the UV/Vis data were observed. This observation suggests that **1** and **3** afford analogous binding modes despite the different acidities exhibited by the phenol and aniline groups.

More mechanistic insights were obtained by ^1H NMR spectroscopy. Increasing amounts of the appropriate tetrabutylammonium salts ($n\text{Bu}_4\text{N}^+ \text{X}^-$) were added to solutions of ligands **1–3** in $[\text{D}_6]$ acetone. Only the results concerning dipyrromethenes **3a** and **3b** substituted with anilines at the α -pyrrole positions will be discussed, because the proton signals of the OH groups of **1a** and **1b** do not appear in their ^1H NMR spectra. Upon the addition of increasing amounts of F^- ions, the ^1H NMR resonances of the dipyrromethene subunit **3b** broadened (Figure 6). On the contrary, no significant changes were observed for the other proton signals of the receptor. Thus, it appears that deprotonation occurs at the pyrrole NH group of the dipyrromethene subunit,^[17] and the rest of the molecule remains unchanged.

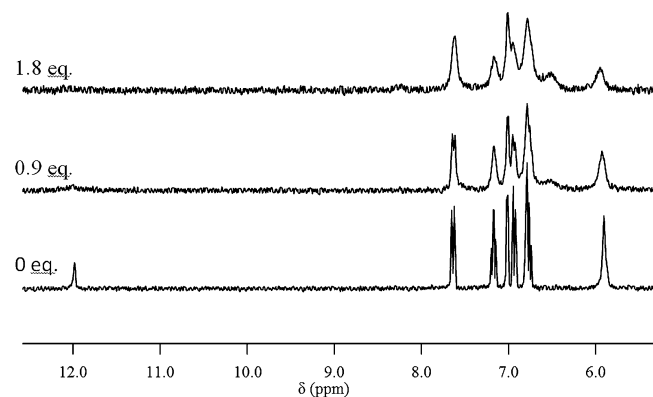


Figure 6. ^1H NMR spectral changes upon titration of receptor **3b** with F^- ions in $[\text{D}_6]$ acetone.

Interactions between Dipyrromethene-Based Receptors and Weakly Basic Anions

For the weakly basic anions, as no noticeable changes were observed in the UV/Vis spectra by applying the same procedure as before, various amounts of tetrabutylammonium chloride, bromide, nitrate, and hydrogen sulfate salts were added to the solutions of receptors **1–3** in $[\text{D}_6]$ acetone.

Surprisingly, upon the addition of a solution of TBACl to a solution of the receptor **3b** in $[\text{D}_6]$ acetone, the NH proton of the dipyrromethene was not affected, and the corresponding resonance remained almost unchanged ($\delta = 11.97$ ppm, $\Delta\delta < 0.1$ ppm; Figure 7). On the contrary, the ^1H NMR resonances of the NH_2 protons and the aromatic protons *ortho* to the NH_2 groups shifted downfield from $\delta = 5.90$ and 6.94 ppm to $\delta = 6.93$ and 7.41 ppm, respectively. These observations exclude the initial assumption concerning the potential insertion of the anion into the cavity of the receptor and reveal a mechanism that involves only the NH_2 protons. The same observations were made with the other ligands **1a**, **1b**, and **3a**. Hence, in all of these cases,

the coordination of the anion does not involve the dipyrromethene subunit. The stoichiometries for the binding of the anions with the studied receptors **1–3** were obtained from Job plots, which indicated the major formation of a 1:1 receptor–anion species for all of the hosts evaluated. Indeed, in any case, the best fit was obtained with a 1:1 model, and the 2:1 binding mode accounted for only 2% of the complexes (see Supporting Information). Titration curves allowed the determination of the corresponding binding constants listed in Table 1 and revealed the formation of weak complexes with association constants of less than 300 M^{-1} .

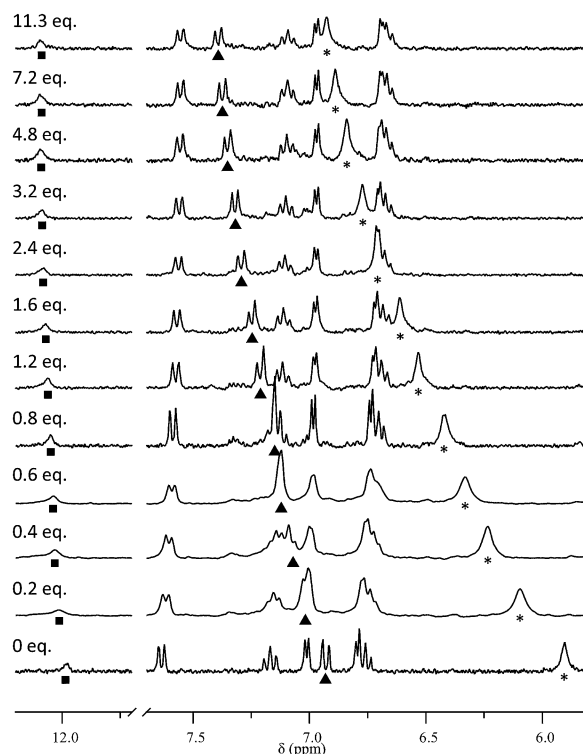


Figure 7. NMR titration of **3b** with tetrabutylammonium chloride in $[\text{D}_6]$ acetone (squares: NH proton of the dipyrromethene; triangles: *ortho* aromatic protons; stars: NH_2 protons).

This observation is quite surprising considering the numerous chelating groups present in the molecules.^[18] In addition, although the association constants are not as high as expected, the anilines proved to be slightly better anion receptors than the corresponding phenols (Table 1, Entries 5–6). This observation could be consistent with the presence of two protons on the amine function; one proton could remain free even if the other one forms an intramolecular hydrogen bond with the dipyrromethene subunit. Finally, the results presented in Table 1 suggest that the *meso* aromatic substituent does not have an influence on the resulting association between the receptors and the anions. Hence, modifications at the *meso* position are possible without modifying the desired properties at the dipyrromethene site.

Very similar observations were made when tetrabutylammonium bromide, nitrate, and hydrogen sulfate salts were added to the solutions of receptors **1–3** in $[\text{D}_6]$ acetone.

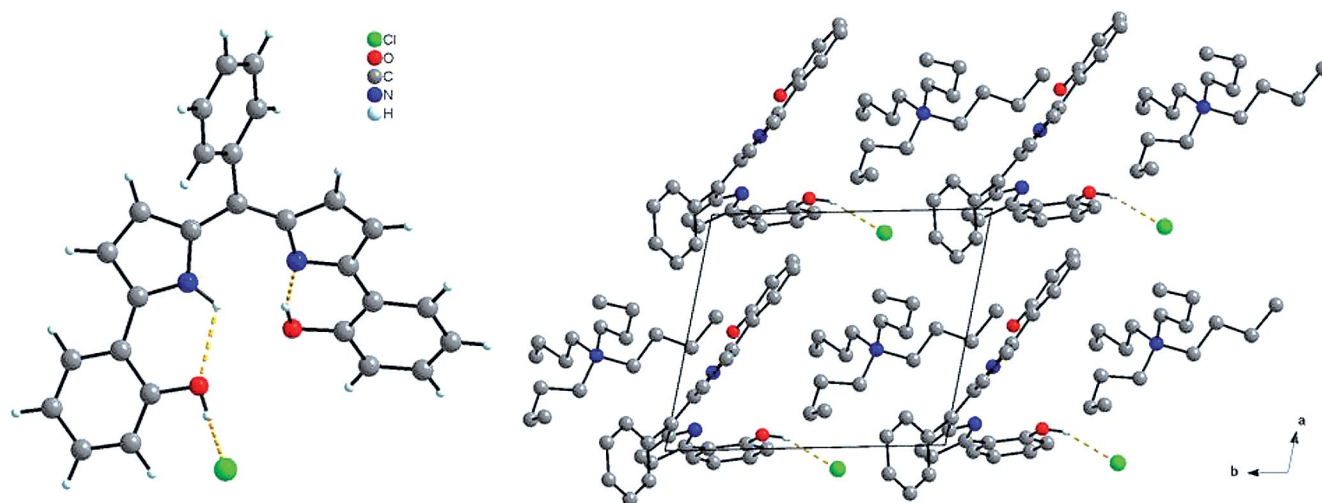


Figure 8. Left: structure of ligand **1a** with a hydrogen bond (orange dashed lines) between one of the phenol groups of the ligand and the chlorine atom. Right: crystal packing of **1a**. Hydrogen atoms not involved in hydrogen bonds are removed for clarity.

To obtain more insight into the actual structure of the 1:1 receptor–anion complex, single crystals of **1a**·Cl[−] were grown by slow concentration of an equimolar dichloromethane solution of **1a** and tetrabutylammonium chloride. Single-crystal X-ray diffraction analyses revealed the H-bonding network of the 1:1 receptor–anion complex (Figure 8).^[19] The molecule crystallized in a non-centrosymmetric space group (triclinic system *P1*). The Flack parameter has been refined to be close to 0 and was then fixed to 0 for the last refinements.

The crystal structure reveals that both phenol groups lie in an *in-in* conformation (Figure 8, left), as the two phenol–OH groups form intramolecular hydrogen bonds with the pyrrole NH group and N atom of the dipyrromethene subunit in the solid state. Thus, the first one involves one phenol group and the sp²-hybridized nitrogen atom of the pyrrole ring, and the second concerns the pyrrole NH group of the second pyrrole ring and the oxygen atom of the second phenol group. As the NH⋯OH hydrogen bond enhances the acidity of the phenol, the free hydrogen atom of this second phenol group can form a hydrogen bond with the free chloride ion [Figure 8, left and right; pyrrole O(H)⋯Cl distance 3.04 Å]. Thus, the weak association constants previously calculated result mainly from the complexation of the anion with one phenol OH group of the receptor. Consequently, the dipyrromethene and the other phenol OH group are not involved in the coordination of the anion.

As the *meso* aromatic substituent of **1a** is not fluorinated, there are no intermolecular hydrogen bonds, and the whole structural cohesion is ensured by weak Coulomb interactions. In addition, owing to the presence of the tetrabutylammonium counteranions, the hosts are well separated from one another with centroid-to-centroid distances of 14.1 and 15.0 Å. The chloride ion is located in the cavity created by the cations and the molecule (Figure 8, right).

Several conclusions can be drawn from the above studies. First, the binding constants of receptor **3b** towards the

tested anions are very similar to those determined with receptor **3a**, which bears a phenyl group. Thus, the expected increased acidity of the pyrrole NH group when a C₆F₅ substituent lies at the *meso* position does not increase the anion-binding affinity. This observation is in agreement with the anion binding occurring only through the aromatic H-bond donor substituent. Second, the association constants calculated for the phenol derivatives are rather low with values that do not exceed 89 M^{−1} (Table 1). Aniline derivatives appear to be slightly more efficient anion receptors than phenols. And third, the nitro-functionalized receptors **2a** and **2b** did not exhibit any complexation of weakly basic anions. This observation is in agreement with the absence of an H-bond donor substituent on the 5-arylpyrrole moiety.

Conclusions

The combined data obtained from the ¹H NMR and UV/Vis spectroscopic titrations and the X-ray structure analyses allowed us to establish the binding mode of *meso*-aryldipyrroin-5,5'-bis(phenol) or -bis(aniline) scaffolds. Thus, independently from the substitution pattern, a 1:1 binding mode was observed in the different cases. With strongly basic anions, the dipyrromethene subunit is involved, and deprotonation at the pyrrole NH position induces a noticeable color change. Conversely, with weakly basic anions, the dipyrromethene only acts as a scaffold, and binding occurs at the aniline or phenol position. Interestingly, it appeared that aniline-substituted dipyrromethenes are slightly better anion receptors than the corresponding phenols. This conclusion was ascertained both by NMR spectroscopy studies and by the fact that very similar association constants (<300 M^{−1}) were measured when the *meso* substituent was a simple phenyl or the electron-withdrawing −C₆F₅ group. Noticeably, only one phenol or aniline group is involved in the complexation, because an internal H-bond network between the other NH₂ or OH group and the dipyrro-

methene moiety prevents the other substituent from participating in the anion recognition. This observation also accounts for the low association constants measured and was definitely acknowledged by the X-crystal structure of **1a**·Cl⁻.

Experimental Section

General: All reactions were performed under argon by using Schlenk techniques. Tetrahydrofuran (THF) was freshly distilled from sodium/benzophenone. Dichloromethane, acetonitrile, and pyrrole were distilled from CaH₂. ZnCl₂ was dried by heating 2 g in thionyl chloride (10 mL) to reflux and removing all of the volatile compounds in vacuo. Benzaldehyde was distilled before use. 2-Chloroanisole and pentafluorobenzaldehyde were purchased from Aldrich and used as received. Analytical TLC was performed on ready-made plates coated with silica gel on aluminum (Merck 60 F₂₅₄). The products were detected by UV light and treatment with permanganate stain followed by gentle heating. Flash chromatography was performed with silica gel (60 Å, particle size 40–63 μm). NMR spectra were recorded with a Bruker ALS 300 MHz spectrometer with a quattro nucleus probe (QNP) in CDCl₃. The ¹H and ¹³C NMR chemical shifts are reported in parts per million (ppm) downfield of tetramethylsilane; the residual solvent signal was used as the internal standard. The ¹⁹F NMR spectra are referenced to CFCl₃. The ¹H NMR information is given in the following format: multiplicity (s singlet, d doublet, t triplet, q quartet, m multiplet, br. broad signal), coupling constants (*J*) in Hertz (Hz), and number of protons. The UV/Vis spectra were recorded with a Shimadzu UVmini-1240 spectrometer. High-resolution mass spectra were recorded with a Bruker MicrOQTOF-Q II XL instrument. The synthesis details for known compounds are reported in the Supporting Information.

Preparation of Dipyrromethenes 2: 2-Aryl-1*H*-pyrrole (1 mmol, 1.0 equiv.) and the aromatic aldehyde (0.5 mmol, 0.5 equiv.) were degassed in a Schlenk tube for 5 min. Degassed anhydrous dichloromethane (20 mL) was then added. Trifluoroacetic acid (TFA; 0.1 mmol, 0.1 equiv.) was added, and the mixture was stirred for the appropriate reaction time. The reaction was monitored by TLC: an aliquot was taken from the reaction, oxidized with 2,3-dichloro-5,6-dicyano-1,4-benzoquinone (DDQ) and developed on the TLC plate. After completion of the reaction, DDQ or *p*-chloranil (0.5 equiv.) was added, and the resulting mixture was further stirred at room temperature for 1 h. The mixture turned rapidly red. The resulting mixture was washed with saturated aqueous NaHCO₃, and the organic layer was filtered through a short pad of Celite[®] with DCM. The crude compound was purified by column chromatography on silica gel.

2a: Reaction performed with benzaldehyde and **6**,^[6] 11 h reaction time, and *p*-chloranil. Chemical yield: 55%. Red solid; m.p. 203–205 °C. *R*_f = 0.25 (DCM/AcOEt, 5:1). ¹H NMR (300 MHz, [D₆]acetone): δ = 12.55 (br. s, 1 H), 7.99 (dd, *J* = 7.8, 1.3 Hz, 2 H), 7.89 (dd, *J* = 8.0, 1.2 Hz, 2 H), 7.80 (ddd, *J* = 7.6, 7.6, 1.3 Hz, 2 H), 7.68 (ddd, *J* = 7.9, 7.9, 1.4 Hz, 2 H), 7.58 (br. s, 5 H), 6.74 (d, *J* = 4.3 Hz, 2 H), 6.67 (d, *J* = 4.3 Hz, 2 H) ppm. ¹³C NMR (75 MHz, [D₆]acetone): δ = 151.2, 150.0, 142.8, 142.7, 137.6, 133.1, 132.0, 131.6, 130.9, 130.8, 130.2, 128.8, 127.3, 124.7, 118.9 ppm. HRMS: calcd. for C₂₇H₁₉N₄O₄ [M + H]⁺ 463.1400; found 463.1401.

2b: Reaction performed with pentafluorobenzaldehyde and **6**, 11 h reaction time, and *p*-chloranil. Chemical yield: 70%. Red solid;

m.p. 208–210 °C. *R*_f = 0.45 (DCM/AcOEt, 5:2). ¹H NMR (400 MHz, [D₆]acetone): δ = 12.19 (s, 1 H), 8.03 (dd, *J* = 7.8, 1.1 Hz, 2 H), 7.93 (dd, *J* = 8.0, 1.0 Hz, 2 H), 7.82 (ddd, *J* = 7.6, 7.6, 1.1 Hz, 2 H), 7.72 (ddd, *J* = 7.9, 7.9, 1.2 Hz, 2 H), 6.91 (d, *J* = 4.4 Hz, 2 H), 6.80 (d, *J* = 4.4 Hz, 2 H) ppm. ¹⁹F NMR (282 MHz, [D₆]acetone): δ = -141.86 (dd, *J* = 21.5, 7.3 Hz, 2 F), -156.06 (t, *J* = 20.5 Hz, 1 F), -164.03 (ddd, *J* = 21.2, 21.2, 5.9 Hz, 2 F) ppm. ¹³C NMR (101 MHz, [D₆]acetone): δ = 153.0, 150.0, 145.9 (br. d, *J* = 246.5 Hz), 142.9 (br. d, *J* = 252.4 Hz), 142.4, 138.8 (br. d, *J* = 251.0 Hz), 133.2, 132.2, 131.3, 129.8, 126.7, 124.8, 124.4, 120.2, 111.8 (dt, *J* = 19.7, 4.2 Hz) ppm. HRMS: calcd. for C₂₇H₁₄F₅N₄O₄ [M + H]⁺ 553.0930; found 553.0931.

Reduction of Nitro Compound 3a:^[7] Under an inert gas were placed **2a** (*M* = 462.5 g mol⁻¹, 231.3 mg, *n* = 0.5 mmol, 1.0 equiv.) and absolute ethanol (20 mL). Palladium on charcoal (Pd/C 10%, *M* = 106.4 g mol⁻¹, *m* = 53.2 mg, *n* = 0.05 mmol, 0.1 equiv.) was added. After homogenization for 5 min, the mixture was heated under reflux, and hydrazine hydrate (*M* = 50.0 g mol⁻¹, *V* = 490 μL, *n* = 10 mmol, 20.0 equiv.) was slowly added. Evolution of gas was rapidly observed. The mixture was stirred under reflux for 2 d and then cooled to room temperature, filtered, and concentrated under reduced pressure. The resulting residue was dissolved in dichloromethane, washed several times with water, dried with Na₂SO₄, and concentrated. The residue was purified by column chromatography with a cyclohexane/dichloromethane mixture. *M* = 402.5 g mol⁻¹, *m* = 157.0 mg, *n* = 0.4 mmol, yield 78%. *R*_f = 0.36 (cyclohexane/DCM, 1:1). ε(497 nm) = 27.8 × 10³ L mol⁻¹ cm⁻¹. Red solid; m.p. 201–207 °C ¹H NMR (300 MHz, [D₆]acetone): δ = 12.24 (br. s, 1 H), 7.61 (dd, *J* = 7.9, 1.4 Hz, 2 H), 7.55 (br. s, 5 H), 7.14 (ddd, *J* = 8.5, 7.2, 1.5 Hz, 2 H), 6.94 (d, *J* = 4.3 Hz, 1 H), 6.90 (dd, *J* = 8.2, 0.9 Hz, 1 H), 6.74 (br. dd, *J* = 7.3, 1.2 Hz, 2 H), 6.61 (d, *J* = 4.3 Hz, 2 H), 5.81 (br. s, 4 H) ppm. ¹³C NMR (75 MHz, [D₆]acetone): δ = 147.4, 141.5, 138.3, 137.1, 131.5, 131.3, 130.0, 129.3, 129.1, 128.8, 128.1, 117.7, 117.5, 117.2, 117.0 ppm. HRMS: calcd. for C₂₇H₂₃N₄ [M + H]⁺ 403.1917; found 403.1908.

Reduction of Nitro Compound 3b: Under an inert gas were placed **2b** (*M* = 462.5 g mol⁻¹, 231.3 mg, *n* = 0.5 mmol, 1.0 equiv.) and anhydrous methanol (20 mL). Palladium on charcoal (Lindlar Pd/C 5%, *M* = 106.4 g mol⁻¹, *m* = 106.4 mg, *n* = 0.05 mmol, 0.1 equiv.) was added. After homogenization for 5 min, hydrogen was bubbled through the medium by using a rubber balloon. The mixture was stirred at room temperature for 15 h, filtered, and concentrated under reduced pressure. The residue was purified by column chromatography with a cyclohexane/dichloromethane mixture as the eluent, and the product was isolated in 76% yield. *M* = 492.5 g mol⁻¹, *m* = 187.1 mg, *n* = 0.38 mmol, yield 76%. Red solid; m.p. 211–215 °C. *R*_f = 0.35 (cyclohexane/DCM, 1:1). ε(544 nm) = 28.8 × 10³ L mol⁻¹ cm⁻¹. ¹H NMR (300 MHz, [D₆]acetone): δ = 11.99 (s, 1 H), 7.65 (dd, *J* = 7.9, 1.2 Hz, 2 H), 7.18 (ddd, *J* = 8.4, 7.2, 1.4 Hz, 2 H), 7.02 (d, *J* = 4.3 Hz, 2 H), 6.94 (d, *J* = 8.1 Hz, 2 H), 6.80 (d, *J* = 4.4 Hz, 2 H), 6.76 (d, *J* = 7.1 Hz, 2 H), 5.91 (br. s, 4 H) ppm. ¹⁹F NMR (282 MHz, [D₆]acetone): δ = -100.86 to -101.10 (m, 2 F), -115.20 (tt, *J* = 2.0, 20.6 Hz, 1 F), -123.04 to -123.28 (m, 2 F) ppm. ¹³C NMR (75 MHz, [D₆]acetone): δ = 153.0, 150.0, 142.4, 133.2, 132.2, 131.3, 129.8, 126.7, 124.8, 124.5, 120.2 ppm. HRMS: calcd. for C₂₇H₁₈F₅N₄ [M + H]⁺ 493.1446; found 493.1446.

Single-Crystal X-ray Diffraction: Single-crystal X-ray studies of **1a**, **2a**, **2b**, and **3b** were performed by using a Gemini diffractometer and the related analysis software.^[20] An absorption correction based on the crystal faces was applied to the data sets (analytical).^[21] All structures were solved by direct methods by using the

SIR97 program^[22] combined with Fourier difference syntheses and refined against F by using the CRYSTALS program with reflections with $I/\sigma(I) > 3$.^[23] All atomic displacement parameters for non-hydrogen atoms were refined with anisotropic terms. The hydrogen atoms were theoretically located on the basis of the conformation of the supporting atom and refined by using a riding model. CCDC-977847 (for **1a**), -977848 (for **2a**), -977849 (for **2b**), and -977850 (for **3b**) contain the supplementary crystallographic data. These data can be obtained free of charge from The Cambridge Crystallographic Data Centre via www.ccdc.cam.ac.uk/data_request/cif.

Supporting Information (see footnote on the first page of this article): Experimental procedures and characterization and titration data.

Acknowledgments

L. C. deeply acknowledges the French Ministry of Higher Education (MESR) for financial support.

- [1] S. El Ghachtouli, K. Wójcik, L. Copey, F. Szydło, E. Framery, C. Goux-Henry, L. Billon, M.-F. Charlot, R. Guillot, B. Andrioletti, A. Aukauloo, *Dalton Trans.* **2011**, 40, 9090–9093.
- [2] a) C. Ikeda, S. Ueda, T. Nabeshima, *Chem. Commun.* **2009**, 2544–2546; b) N. Sakamoto, C. Ikeda, M. Yamamura, T. Nabeshima, *J. Am. Chem. Soc.* **2011**, 133, 4726–4729; c) S. Rausaria, A. Kamadulski, N. P. Rath, L. Bryant, Z. Chen, D. Salvemini, W. L. Neumann, *J. Am. Chem. Soc.* **2011**, 133, 4200–4203; d) M. Yamamura, H. Takizawa, N. Sakamoto, T. Nabeshima, *Tetrahedron Lett.* **2013**, 54, 7049–7052; e) M. Yamamura, M. Albrecht, M. Albrecht, Y. Nishimura, T. Arai, T. Nabeshima, *Inorg. Chem.* **2014**, 53, 1355–1360.
- [3] H. Kim, A. Burghart, M. B. Welch, J. Reibenspies, K. Burgess, *Chem. Commun.* **1999**, 1888–1890.
- [4] R. D. Rieth, N. P. Mankad, E. Calimano, J. P. Sadighi, *Org. Lett.* **2004**, 6, 3981–3983.
- [5] M. Alešković, N. Basarić, I. Halasz, X. Liang, W. Qin, K. Minarić-Majerski, *Tetrahedron* **2013**, 69, 1725–1734.
- [6] H. Yuefei, S. Changwei, W. Xinyan, X. Jimin, Z. Rui, CN101817774, **2010**.
- [7] M. Bernátkova, B. Andrioletti, V. Král, E. Rose, J. Vaissermann, *J. Org. Chem.* **2004**, 69, 8140–8143.
- [8] The reduction of **2b** with hydrazine hydrate and palladium on charcoal failed to produce the desired dianiline compound **3b**. Side reactions involving the substitution of several fluorine atoms were observed, and no trace of the desired product was identified.
- [9] Empirical formula: $C_{27}H_{19}N_4O_4$; molecular weight: 463.5 $g\ mol^{-1}$; crystal system: monoclinic; space group: $C2/c$; $a = 13.177(1)\ \text{Å}$; $b = 12.3257(7)\ \text{Å}$; $c = 14.932(1)\ \text{Å}$; $\beta = 109.23(1)^\circ$; $V = 2289.9(4)\ \text{Å}^3$; crystal description: cube; crystal color: red; crystal size: $0.288 \times 0.306 \times 0.455\ \text{mm}$; $Z = 4$; $T = 293\ \text{K}$; $d = 1.344$; $\mu = 0.093\ \text{mm}^{-1}$; number of independent reflections: 2686; $R_{\text{int}} = 0.016$; $R(F) = 0.0439$; $R_w(F) = 0.0465$; $S = 1.17$; $\Delta\rho_{\text{min}} = -0.28\ e^{-\text{Å}^{-3}}$; $\Delta\rho_{\text{max}} = +0.19\ e^{-\text{Å}^{-3}}$; number of reflections used: 1774; number of refined parameters: 161; absorption correction: analytical.
- [10] Empirical formula: $C_{27}H_{14}F_5N_4O_4$; molecular weight: 553.4 $g\ mol^{-1}$; crystal system: monoclinic; space group: $C2/c$; $a = 13.348(2)\ \text{Å}$; $b = 12.604(2)\ \text{Å}$; $c = 14.848(4)\ \text{Å}$; $\beta = 104.44(2)^\circ$; $V = 2419.2(8)\ \text{Å}^3$; crystal description: cube; crystal color: orange; crystal size: $0.288 \times 0.306 \times 0.455\ \text{mm}$; $Z = 4$; $T = 293\ \text{K}$; $d = 1.519$; $\mu = 0.130\ \text{mm}^{-1}$; number of independent reflections: 2865; $R_{\text{int}} = 0.021$; $R(F) = 0.0488$; $R_w(F) = 0.0624$; $S = 1.03$; $\Delta\rho_{\text{min}} = -0.27\ e^{-\text{Å}^{-3}}$; $\Delta\rho_{\text{max}} = +0.32\ e^{-\text{Å}^{-3}}$; number of reflections used: 1811; number of refined parameters: 183; absorption correction: analytical.
- [11] J.-Y. Shin, B. O. Patrick, D. Dolphin, *CrystEngComm* **2008**, 10, 960–962.
- [12] Empirical formula: $C_{27}H_{17}F_5N_4$; molecular weight: 492.5 $g\ mol^{-1}$; crystal system: orthorhombic; space group: $Pbca$; $a = 45.297(5)\ \text{Å}$; $b = 10.549(5)\ \text{Å}$; $c = 9.291(5)\ \text{Å}$; $V = 4440(3)\ \text{Å}^3$; crystal description: cube; crystal color: dark purple; crystal size: $0.200 \times 0.241 \times 0.289\ \text{mm}$; $Z = 8$; $T = 293\ \text{K}$; $d = 1.473$; $\mu = 0.118\ \text{mm}^{-1}$; number of independent reflections: 5290; $R_{\text{int}} = 0.073$; $R(F) = 0.0607$; $R_w(F) = 0.0719$; $S = 1.10$; $\Delta\rho_{\text{min}} = -0.25\ e^{-\text{Å}^{-3}}$; $\Delta\rho_{\text{max}} = +0.28\ e^{-\text{Å}^{-3}}$; number of reflections used: 1865; number of refined parameters: 325; absorption correction: multiscan.
- [13] a) P. A. Gale, *Chem. Soc. Rev.* **2010**, 39, 3746–3771; b) M. Wenzel, J. R. Hiscock, P. A. Gale, *Chem. Soc. Rev.* **2012**, 41, 480–520.
- [14] a) C. B. Black, B. Andrioletti, A. C. Try, C. Ruiperez, J. L. Sessler, *J. Am. Chem. Soc.* **1999**, 121, 10438–10439; b) X. Yong, M. Su, W. Wang, Y. Yan, J. Qu, R. Liu, *Org. Biomol. Chem.* **2013**, 11, 2254–2257.
- [15] a) J. L. Sessler, E. Katayev, G. Dan Pantos, P. Scherbakov, M. D. Reshetova, V. N. Khrustalev, V. M. Lynch, Y. A. Ustyniuk, *J. Am. Chem. Soc.* **2005**, 127, 11442–11446.
- [16] D. H. Lee, K. H. Lee, J.-I. Hong, *Org. Lett.* **2001**, 3, 5–8.
- [17] S. Camiolo, P. A. Gale, M. B. Hursthouse, M. E. Light, *Org. Biomol. Chem.* **2003**, 1, 741–744.
- [18] P. Dydio, D. Lichosyt, T. Zieliński, J. Jurczak, *Chem. Eur. J.* **2012**, 18, 13686–13701.
- [19] Empirical formula: $C_{43}H_{56}Cl_1N_3O_2$; molecular weight: 682.4 $g\ mol^{-1}$; crystal system: triclinic; space group: $P1$; $a = 8.8094(6)\ \text{Å}$; $b = 10.4348(6)\ \text{Å}$; $c = 11.2241(8)\ \text{Å}$; $\alpha = 100.167(5)^\circ$; $\beta = 91.017(5)^\circ$; $\gamma = 102.103(5)^\circ$; $V = 991.39(11)\ \text{Å}^3$; crystal description: plate; crystal color: purple; crystal size: $0.089 \times 0.364 \times 0.472\ \text{mm}$; $Z = 1$; $T = 293\ \text{K}$; $d = 1.143$; $\mu = 0.134\ \text{mm}^{-1}$; number of independent reflections: 6373; $R_{\text{int}} = 0.020$; $R(F) = 0.0537$; $R_w(F) = 0.0605$; $S = 1.08$; $\Delta\rho_{\text{min}} = -0.21\ e^{-\text{Å}^{-3}}$; $\Delta\rho_{\text{max}} = +0.37\ e^{-\text{Å}^{-3}}$; Flack parameter: 0.0; number of reflections used: 4205; number of refined parameters: 443; absorption correction: analytical.
- [20] *CrysAlisPro*, v. 1.171.33.46 (rel. 27-08-2009 CrysAlis171.NET), Oxford Diffraction Ltd. **2009**.
- [21] J. de Meulenaer, H. Tompa, *Acta Crystallogr.* **1965**, 19, 1014–1018.
- [22] M. Altomare, C. Burla, M. Camalli, G. L. Casciarano, C. Giacovazzo, A. Guagliardi, A. G. G. Moliterni, G. Polidori, R. Spagna, *J. Appl. Crystallogr.* **1999**, 32, 115–119.
- [23] D. J. Watkin, C. K. Prout, J. R. Carruthers, P. W. Betteridge, *CRYSTALS Issue 11*, Chemical Crystallography Laboratory, Oxford, **1999**.

Received: April 18, 2014
Published Online: June 24, 2014